2024 IEEE International Symposium on Electromagnetic Compatibility, Signal & Power Integrity (EMC+SIPI) | 979-8-3503-6039-4/24/$31.00 ©2024 IEEE | DOI: 10.1109/EMCSIPI49824.2024.10705580

Design of Waveguide Probe for EMI Characterization of DDR5 SODIMM

Xiangrui Su[#1], Junho Joo[#2], Minsu Lee[*3], Jeongho Ju[*4], Hyunsik Kim[*5], Taeil Bae[*6], Haekang Jung[*7] and Chulsoon Hwang[#8]
[#]*EMC Laboratory, Missouri University of Science and Technology*, Rolla, MO, USA
[*]*System Integrity Group, SK hynix Inc*., Icheon-si, Gyeonggi-do, South Korea
[1]suxia@mst.edu

***Abstract*—In the latest portable electronic devices, 5th generation double data rate small outline dual in-line memory modules (DDR5 SODIMMs) are more and more used and have been identified as one of the critical electromagnetic interference (EMI) noise sources that could cause RF desensitization. In this paper, the radiation mechanism of DDR5 SODIMM deployed in a laptop is identified and investigated based on near-field scanning. It was found that a cavity formed by the SODIMM and the main board can generate strong radiation around 2.4 GHz due to their dimensions, which overlap with the Wi-Fi band. To quantify the radiation from the cavity, a waveguide probe was designed to perform quick measurements. The performance of the proposed probe showed better sensitivity compared to conventional loop probes. The designed probe was built and used to characterize 4 different SODIMMs from 3 manufacturers. The waveguide probe-measured noise was proportional to the coupled power on the Wi-Fi antenna with an accuracy of 3 dB.**

Keywords—RFI, DDR5 SODIMM, near-field scanning, waveguide probe

I. Introduction

Because of the escalating speed and intricacy of modern electronic technologies, the internal architectures of mobile platforms, including phones and laptops, are increasingly compact. The proximity between antennas and high-speed modules leads to the potential pickup of electromagnetic noise by radio frequency (RF) antennas [1]-[2]. This in turn results in RF desensitization on the receiving antennas. Electromagnetic interference (EMI) issues stem from various noise sources, such as solid-state drives (SSDs) [3], connectors [4]-[5], heatsinks [6], cameras [7]-[8], integrated circuit (IC) chips [9] and flexible flat cables [10]-[12].

Because of the increased bandwidth, higher capacity, and improved efficiency, DDR5 dynamic random-access memory (DRAM) is more and more used. 5th generation double data rate small outline dual in-line memory module (DDR5 SODIMM) inherits the benefits of DDR5 technology and is tailored to fit the size and power constraints of portable and small form factor devices. But this high-speed module could become an RF noise source, especially in compact devices like mobiles and laptops. Therefore, detecting and analyzing RFI issues at a component level is beneficial and important.

It is not new that DRAM could be a serious radio frequency interference (RFI) noise source. As reported in [13]-[15], the RFI issue on DRAM was found and analyzed in former generations. However, as a common RFI debug method, near-field scanning technology was widely used in identifying and quantifying the noise source not only in DRAM analysis [13]-[14], but also in many other applications [3], [16]-[18]. Near-field scanning allows for a detailed examination of the electromagnetic characteristics of a system, helping engineers and technicians locate and mitigate issues related to electromagnetic radiation, coupling, and interference. But it is usually very time-consuming and equipment-demanding. The near filed scanning was performed on four different SODIMMs and all their near field distribution show the edge radiation at around 2.4 GHz. After the noise mechanism is well studied, a quick measurement method instead of near-field scanning to quantify the RF noise from SODIMM will be greatly helpful for the EMC engineers, especially in the development stage when there are many models to be tested. To deploy the quick measurements, a large probe is needed to cover the entire edge of the SODIMM. Usually, the loop probe cannot be too large because of bandwidth limitation caused by increased parasitic parameters. However, a waveguide probe is a good option that can be large enough to cover the SODIMM edge without bandwidth restriction.

In this paper, the noise radiation mechanism of the SODIMM mounted on a main board is understood based on near-field scanning. Then based on the understanding, a waveguide probe is designed to pick up the noise efficiently and fast. The measured noise using the proposed waveguide probe is compared to the coupled power at the embedded Wi-Fi antenna with 4 different cases. The waveguide probe's performance is also compared to conventional loop probes in terms of sensitivity and stability. Iconic band noise was observed in both near field from SODIMM and coupled power on the Wi-Fi antenna, which proved the edge radiation from SODIMM is the most dominant RF noise source. To quickly quantify the magnitude of the edge radiation, a waveguide probe was designed, fabricated, and validated under four different SODIMM cases.

II. SODIMM Radiation Mechanism

The device under test in this paper is the DDR5 SODIMM situated on a laptop, illustrated in Fig. 1. A script was running to control the throughput between the SODIMM and the motherboard, which was used to avoid the laptop goes to idle status.

Firstly, H-field near-field scanning was performed above the SODIMMs. Fig. 2 illustrates the schematic of the near-field scanning measurement setup. A broadband EMC H-field probe

This paper was result of the research project supported by SK hynix Inc.

with a 20 mm diameter loop size was affixed to a robot arm. The robot arm can rotate the probe by 90 degrees, allowing for the measurement of two orthogonal field components, H_x and H_y. The probe's output was connected to a spectrum analyzer (SA) through two cascaded low-noise amplifiers. Before the scanning process, probe calibration was conducted using a coplanar waveguide (CPWG), following the methodology outlined in [19].

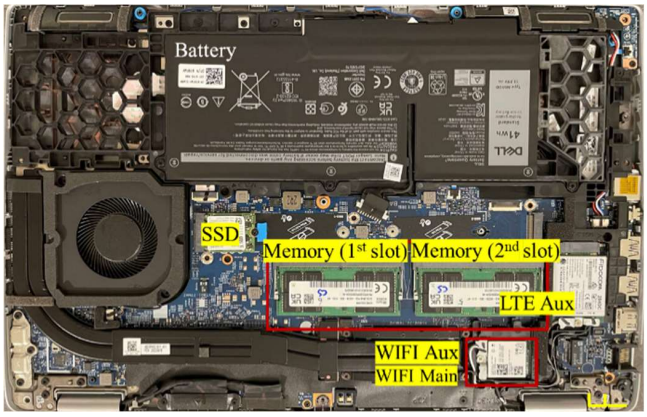

Fig. 1. DRAM SODIMM platform.

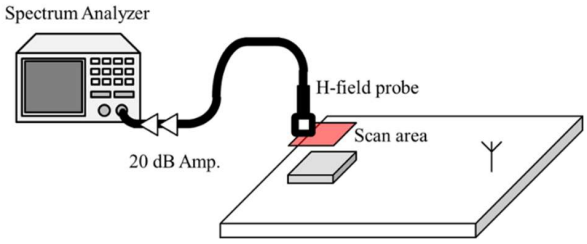

Fig. 2. Diagram of near-field scanning setup.

As illustrated in Fig. 3. The SODIMM, the laptop's main board, and the connector form a cavity structure with the connector side shorted (short side) and the other three sides open (open side). The dimensions of the SODIMM are 70 mm in length and 30 mm in width. The standing wave can be formed along the width direction because the connector side is shorted and causes reflection. The first cavity resonance frequency f_1 can be calculated to be 2.5 GHz by (1), where ε and μ are the permittivity and permeability of the dielectric (air in this case), m is the mode number along the width direction, w is the width of the cavity and f_m is the resonance frequency of mode m.

$$f_m = \frac{1}{2\sqrt{\varepsilon\mu}} \times \left(\frac{m}{2 \times w}\right) \quad (1)$$

Because one side boundary is open and thus the first resonance is a quarter-wavelength resonance. The resonance frequency is close to 2.4 GHz Wi-Fi bandwidth and could be one noise source that causes RFI issues.

The H-field scanning results, with a scanning height of 5.3 mm, are shown in Fig. 4. The scanning results show strong radiation along the edge of the SODIMM: H_x along the width direction and H_y along the length direction. The connector side of the SODIMM is connected to the laptop main board through the DRAM connector and socket. There is a hot spot around the center of the connector side because there is a notch with no pins in the middle of the DRAM connector.

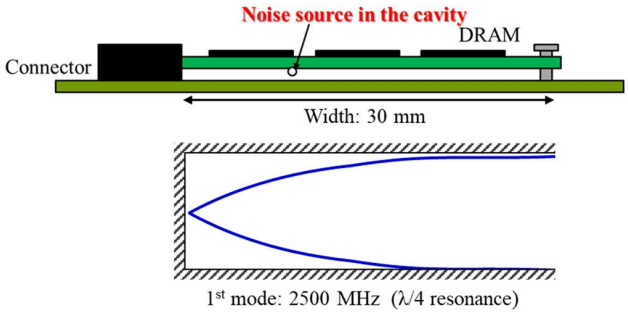

Fig. 3. Cavity structure formed by SODIMM and main board [20].

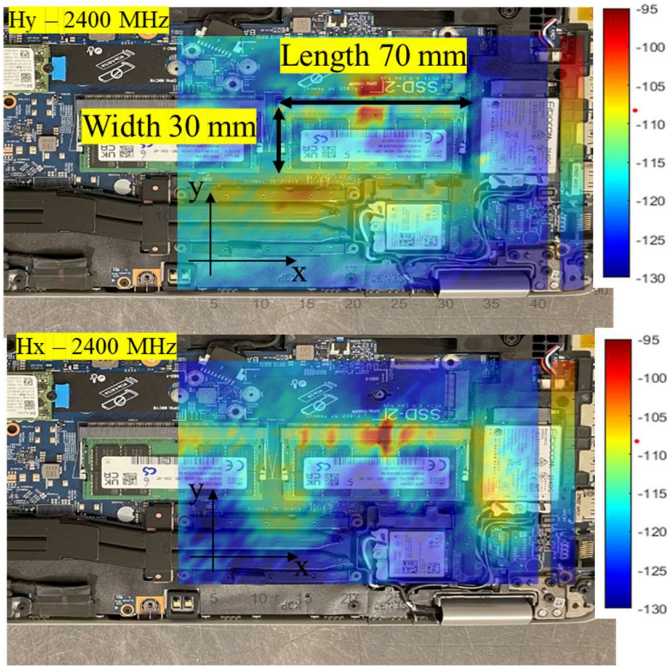

Fig. 4. Near-field scanning result above SODIMM.

The spectrum of the near field is compared with that of coupled noise on the embedded Wi-Fi antenna is shown in Fig. 5. It clearly shows that the edge radiation from the SODIMM has a strong noise within the frequency band from 2390 MHz to 2400 MHz, which is responsible for the same band on the coupled noise on the Wi-Fi antenna. It should be noted that the SODIMMs tested in this paper had already been engineered to avoid interference with the Wi-Fi band by lowering the fundamental frequency of the DRAM. The noise from 2390 MHz to 2400 MHz wouldn't affect the Wi-Fi sensitivity because it is out of the band of Wi-Fi. A new measurement method that can replace time-consuming near-field scanning is proposed in the next section, and the SODIMM noise in the frequency range of 2390 MHz to 2400 MHz is used to evaluate the proposed method assuming that the probe performance

would exhibit similar performance in the actual Wi-Fi band (2400 MHz – 2500MHz).

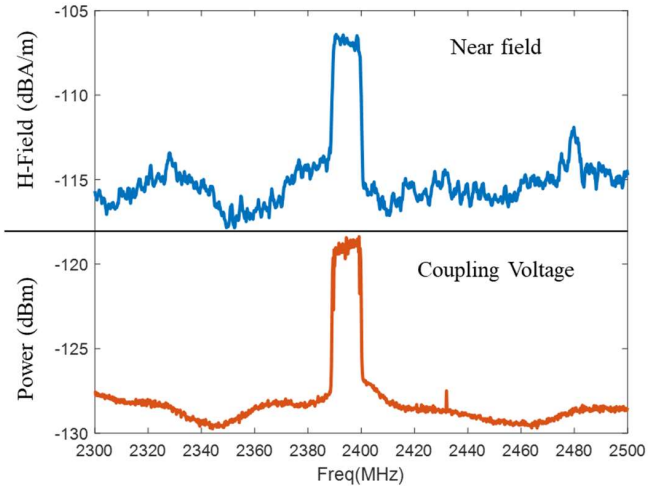

Fig. 5. Spectrum comparison between the measured near field (edge radiation) and coupled noise on the Wi-Fi antenna.

III. Waveguide Probe

A waveguide probe is a device used in the field of electromagnetic wave propagation and communication systems. The rectangular aperture of the waveguide probe is suitable to capture the edge radiation. The waveguide probe consists of two parts: a waveguide and a coaxial feeding as depicted in Fig. 6. The main body of the waveguide probe is the waveguide itself with one side open for receiving signals and the other side short. Inside the waveguide, there is a monopole extended from the inner pin of the coaxial feeding responsible for receiving electromagnetic waves.

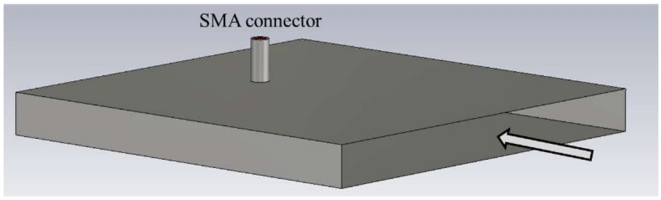

Fig. 6. Illustration of waveguide probe with SMA connector.

The dimensions of the waveguide probe are shown in Fig. 7. The broad wall width of the waveguide probe is set to 70 mm for two reasons: 1) To make the cut-off frequency 2.1 GHz which is lower than the Wi-Fi frequency range, and 2) As wide as the SODIMM to capture all the edge radiation. The incident wave and the wave reflected by the short side waveguide wall form a standing wave inside the waveguide. The location of the receiving monopole antenna is optimized to be 30 mm away from the short side where the wave peak of the standing wave is at 2.4 GHz as shown in Fig. 8.

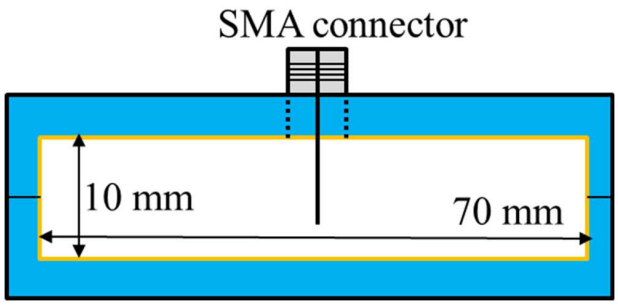

Fig. 7. Cross-section of waveguide probe.

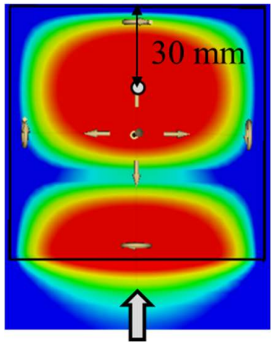

Fig. 8. Standing wave inside the waveguide probe.

The designed waveguide was built using a 3D-printed plastic waveguide wall coated by copper tapes. To rule out the potential inhomogeneous dielectric effect that could be introduced by the 3D printing material. The copper tape was coated inside the 3D-printed wall instead of the outside. The monopole was built by a short copper wire connected to the inner pin of an SMA connector, whose reference plane is the waveguide. This waveguide probe was designed to work at 2.4 GHz, but it's easy to be optimized to work at 5 GHz by simply changing the location of the monopole structure.

Fig. 9. Side view and front view of the waveguide probe.

IV. Measurement

To check the effectiveness and validity of the waveguide probe to quantify the SODIMM noise, 4 cases were measured including 4 SODIMMs from three different manufacturers. Then the waveguide probe-measured power and the coupled power on the laptop's Wi-Fi antenna are compared.

The measurement setup is demonstrated in Fig. 10. All measurements were conducted inside an EMI chamber to isolate the DUT from the environmental noise. A script was running during the measurement to avoid the SODIMM working in idle status. The waveguide probe was fixed on a probe holder. The probe was located close to the broad edge of the SODIMM. The laptop was on an adjustable height base to make the open aperture of the waveguide probe at the same height as the SODIMM surface. The waveguide probe was connected to the SA after two cascaded low-noise amplifiers. Then the same measurement environment was kept when measuring the coupled power on the laptop's Wi-Fi antenna. To reduce the error introduced by the instability of the SODIMM noise, average mode was used to measure the average power of 100 sweeps.

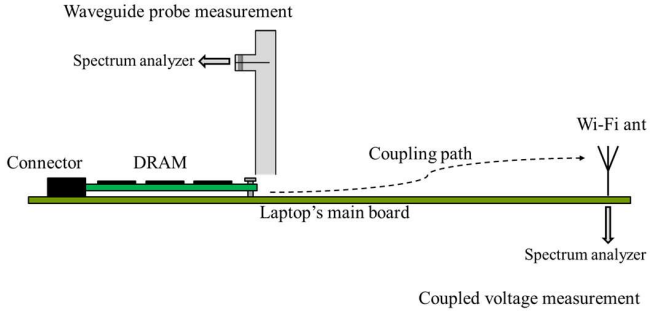

Fig. 10. Diagram of waveguide probe measurement and coupled power measurement.

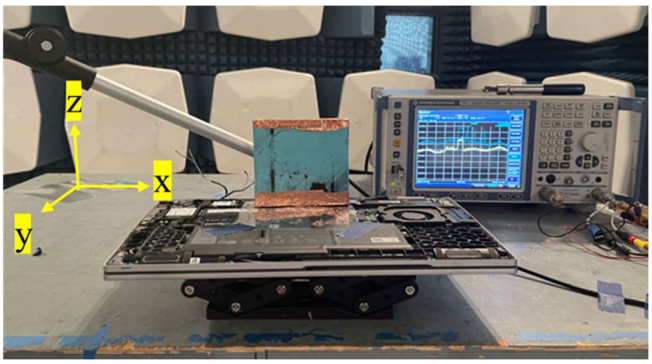

Fig. 11. Photograph of waveguide probe measurement setup; the probe was placed above the SODIMM.

As the radiation mechanism is associated with the physical dimensions of SODIMM, all DDR5 SODIMM are expected to have the same behavior (edge radiation). Consequently, the waveguide probe output (near-field of SODIMM) should be proportional to the coupled power on the Wi-Fi antenna. The measurement results are depicted in Fig. 12. 4 cases were measured with the waveguide probe and compared to the coupled power on the Wi-Fi antenna. The horizontal axis shows the averaged coupled power on the Wi-Fi antenna from 2390 MHz to 2400 MHz and the vertical axis shows the waveguide probe measurement average receiving power in the same band for each case. The red line is a 45-degree slope baseline fitted by 4 measured cases. The error margin was ±1.5 dB.

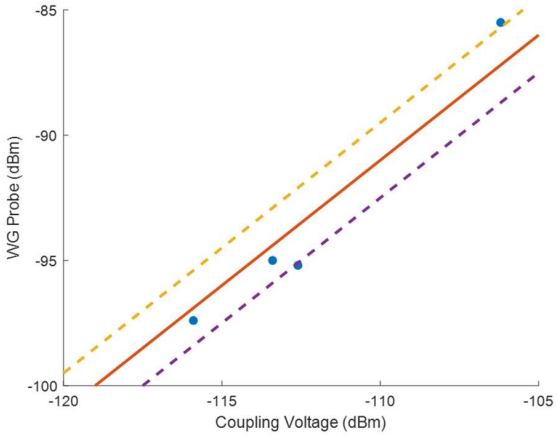

Fig. 12. Waveguide probe output vs. coupled noise power on the Wi-Fi antenna for 4 different cases.

The sensitivity and stability of the probe are two key factors for accurate measurement. Better sensitivity means the probe could capture weaker noise, i.e., better probe factor. Stability here represents the power variation received by the probe with a slight spatial offset in the measurement location. Because in practical measurement, it is hard to keep the same probing location in every measurement, therefore the measurement results must not be too sensitive to the measurement location.

Besides the waveguide probe, a 20 mm diameter loop probe and a 10 mm diameter loop probe were used to measure the SODIMM, and the results are compared against the waveguide probe in terms of sensitivity and stability. When using the loop probes to quantify the SODIMM noise, the probes were located above the middle of the open edge of SODIMM as shown in Fig. 13. The sensitivity comparison between three probes was conducted by measuring the same SODIMM using three probes. It should be noted that the effective probing height between the three probes is different, which is the case in the practical measurement. The stability is checked by comparing the received power before and after moving the probes by 10 mm along the x-axis as shown in Fig. 14. The relative received power difference in decibels is defined as the stability in this paper.

The comparison between the three probes is summarized in Table 1. Intuitively, the waveguide probe's sensitivity is higher than the loop probes because it has a larger aperture area than the loops. It's also worth mentioning that the waveguide probe picks up the E-field while the loop probe picks up the H-field. The broader aperture of the waveguide probe makes its receiving result better representing the average field along the total edge instead of at a point that is measured by the loop probes.

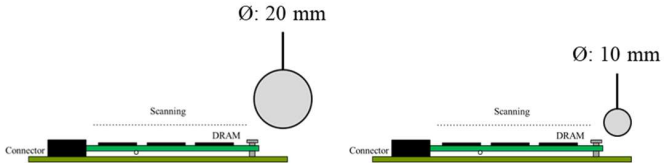

Fig. 13. Illustration of loop probe probing location.

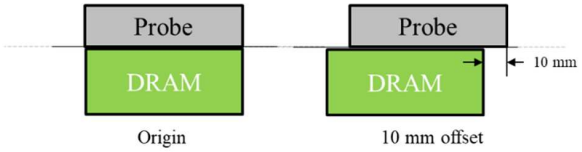

Fig. 14. Spatial offset in stability measurement.

TABLE I. THREE PROBES COMPARISION

	Probe Type		
	Waveguide Probe	***20mm Loop Probe***	***10mm Loop Probe***
Recived power from a common source	-85.5 dBm	-98.9 dBm	-107.5 dBm
Stability	2.3 dB	3.6 dB	2.0 dB

V. CONCLUSION

This paper introduces the design of a waveguide probe that can quickly quantify the noise level generated by DDR5 SODIMM. This designed waveguide probe was validated by measuring 4 cases including 4 SODIMMs from different SODIMM manufacturers and achieved less than ±1.5 dB error. Furthermore, given the limited testing performed described herein, this waveguide probe was validated to be more sensitive than the common 10 cm and 20 cm loop probes and exhibited stability similar to the loop probe.

REFERENCES

[1] L. Zhang et al., "Radio-Frequency Interference Estimation for Multiple Random Noise Sources," *IEEE Transactions on Electromagnetic Compatibility*, vol. 64, no. 2, pp. 358-366.

[2] C. Hwang and J. Fan, "Modeling and Mitigation of Radio Frequency Interference for Wireless Devices," *IEEE Electromagnetic Compatibility Magazine*, vol. 12, no. 1, pp. 87-92.

[3] X. Su, W. Huang, J. Cho, J. Paek, and C. Hwang, "Near Field Scanning-Based EMI Radiation Root Cause Analysis in an SSD," *2023 IEEE Symposium on Electromagnetic Compatibility & Signal/Power Integrity (EMC+SIPI)*, 2023, pp. 202-206.

[4] L. Zhang et al., "Accurate RFI prediction of 3D non-planar connector with half magnetic dipole pattern," *2019 Joint International Symposium on Electromagnetic Compatibility, Sapporo and Asia-Pacific International Symposium on Electromagnetic Compatibility (EMC Sapporo/APEMC)*, 2019, pp. 770-773.

[5] Y. Sun, H. Lin, B. Tseng, D. Pommerenke, and C. Hwang, "Mechanism and Validation of USB 3.0 Connector Caused Radio Frequency Interference," *IEEE Trans. on Electromagnetic Compatibility*, vol. 62. no.4, pp.1169-1178.

[6] Huang, Qiaolei, et al. "Reciprocity theorem based RFI estimation for heatsink emission," *2019 IEEE International Symposium on Electromagnetic Compatibility, Signal & Power Integrity (EMC+ SIPI)*. IEEE, 2019, pp. 590-594.

[7] Z. Sun, Y. Wang, W. Lee, K. Wu, and D. Kim, "Radiated Noise Source Characterization Based on Magnitude-Only Near Field," *2021 IEEE International Joint EMC/SI/PI and EMC Europe Symposium*, 2021, pp. 376-380.

[8] Z. Sun, Y. Wang, and D. Kim, "System-level Validation of Radiated Noise Source Characterization Using Only Near Field Magnitude Information," *IEEE Letters on Electromagnetic Compatibility Practice and Applications*.

[9] C. Wu, Z. Sun, Q. Huang, Y. Wang, J. Fan, and J. Zhou, "A Method to Extract Physical Dipoles for Radiating Source Characterization and Near Field Coupling Estimation," *2019 IEEE International Symposium on Electromagnetic Compatibility, Signal & Power Integrity (EMC+SIPI),* 2019, pp. 580-583.

[10] X. Yan et al., "EMI Investigation and Mitigation of Flexible Flat Cables and Connectors," *2021 IEEE International Joint EMC/SI/PI and EMC Europe Symposium*, 2021, pp. 515-519.

[11] Y. Zhong et al., "Measurement-Based Quantification of Buzz Noise in Wireless Devices," *2019 Joint International Symposium on Electromagnetic Compatibility, Sapporo and Asia-Pacific International Symposium on Electromagnetic Compatibility (EMC Sapporo/APEMC),* 2019, pp. 552-555.

[12] G. Tsintsadze, H. Manoharan, D. Beetner, D. Commerou, B. Booth and K. Martin, "Predicting Radiated Emissions from an Electrical Drive System," *2023 Joint Asia-Pacific International Symposium on Electromagnetic Compatibility and International Conference on ElectroMagnetic Interference & Compatibility (APEMC/INCEMIC)*, 2023, pp. 1-4.

[13] B. Kim et al., "Near-Field EMI Analysis of LPDDR5 DRAM at idle mode," *2023 IEEE Symposium on Electromagnetic Compatibility & Signal/Power Integrity (EMC+SIPI)*, 2023, pp. 311-314.

[14] Pilssoo Lee, Junho Lee, Dae-kun Yoon, Jaehoon Choi, and Sungjoo Hong, "Analysis of DRAM EMI dependence on data pattern and power delivery design using a near-field EMI scanner," *2008 Asia-Pacific Symposium on Electromagnetic Compatibility and 19th International Zurich Symposium on Electromagnetic Compatibility*, pp. 271-274.

[15] S. Moon, S. Kim, D. -C. Kim, D. Yi, S. -B. Lee, and J. Shin, "Analysis and Estimation on EMI Effects in AP-DRAM Interface for a Mobile Platform," *2016 IEEE 66th Electronic Components and Technology Conference (ECTC)*, 2016, pp. 1329-1334.

[16] S. Xia, H. Wang, Y. Wang, Z. Wu, C. Hwang, and J. Fan, "Dipole-Moment-Based Reciprocity for Practical Desensitization Identification and Mitigation," *IEEE Transactions on Electromagnetic Compatibility*, vol. 65, no. 4, pp.

[17] Q. Huang, F. Zhang, T. Enomoto, J. Maeshima, K. Araki, and C. Hwang, "Physics-Based Dipole Moment Source Reconstruction for RFI on a Practical Cellphone," *IEEE Transactions on Electromagnetic Compatibility*, vol. 59, no. 6, pp. 1693-1700.

[18] S. Xia *et al*., "RFI Estimation for Multiple Noise Sources Due to Modulation at a Digital Mic Using Diople Moment Based Reciprocity," *2020 IEEE International Symposium on Electromagnetic Compatibility & Signal/Power Integrity (EMCSI)*, 2020, pp. 1-5.

[19] J. Zhang, K. W. Kam, J. Min, V. V. Khilkevich, D. Pommerenke, and J. Fan, "An Effective Method of Probe Calibration in Phase-Resolved Near-Field Scanning for EMI Application," *IEEE Transactions on Instrumentation and Measurement*, vol. 62, no. 3, pp. 648-658.

[20] J. Joo et al., "Modeling of RF Interference Caused by Solid-State Drive Noise," *2022 Asia-Pacific International Symposium on Electromagnetic Compatibility (APEMC)*, 2022, pp. 685-687